

## CAN GAMMA-RAY BURST JETS BREAK OUT THE FIRST STARS?

YUDAI SUWA<sup>1,2</sup> AND KUNIHITO IOKA<sup>3</sup>

*Draft version September 18, 2018*

### ABSTRACT

We show that a relativistic gamma-ray burst (GRB) jet can potentially pierce the envelope of very massive first generation star (Population III; Pop III) by using the stellar density profile to estimate both the jet luminosity (via accretion) and its penetrability. The jet breakout is possible even if the Pop III star has a supergiant hydrogen envelope without mass loss, thanks to the long-lived powerful accretion of the envelope itself. While the Pop III GRB is estimated to be energetic  $E_{\gamma, \text{iso}} \sim 10^{55}$  erg, the supergiant envelope hides the initial bright phase into the cocoon component, leading to a GRB with a long duration  $\sim 1000(1+z)$  sec and an ordinary isotropic luminosity  $\sim 10^{52}$  erg s<sup>-1</sup> ( $\sim 10^{-9}$  erg cm<sup>-2</sup> s<sup>-1</sup> at redshift  $z \sim 20$ ). The neutrino-annihilation is not effective for Pop III GRBs because of a low central temperature, while the magnetic mechanism is viable. We also derive analytic estimates of the breakout conditions, which are applicable to various progenitor models. The GRB luminosity and duration are found to be very sensitive to the core and envelope mass, providing possible probes of the first luminous objects at the end of the high redshift dark ages.

*Subject headings:* Cosmology: dark ages, reionization, first stars – Gamma-ray burst: general — Stars: general

### 1. INTRODUCTION

The ancient era of the first generation stars (Population III; Pop III) – the end of the dark age – is still an unexplored frontier in the modern cosmology (Barkana & Loeb 2001; Bromm & Larson 2004; Ciardi & Ferrara 2005). The first star formation from the metal free gas has a crucial influence on the subsequent cosmic evolution by producing ionizing photons and heavy elements. Although the theoretical studies are recently developed by the numerical simulations, the faint Pop III objects are difficult to observe even with the future technology.

Gamma-Ray Bursts (GRBs) are potentially powerful probes of the Pop III era. In fact, GRB 090423 got the highest redshift  $z = 8.2$  ever seen (e.g., Tanvir et al. 2009; Salvaterra et al. 2009; Chandra et al. 2010), beyond any quasars or galaxies and previous GRB 080913 at  $z = 6.7$  (Greiner et al. 2009) and GRB 050904 at  $z = 6.3$  (Kawai et al. 2006; Totani et al. 2006). The GRBs are presumed to manifest the gravitational collapse of a massive star – a collapsar – to a black hole with an accretion disk, launching a collimated outflow (jet) with a relativistic speed (MacFadyen & Woosley 1999). The massive stars quickly die within the Pop III era. The GRBs, the most luminous objects in the Universe, are detectable in principle out to redshifts  $z \sim 100$  (Lamb & Reichart 2000), while their afterglows are observable up to  $z \sim 30$  (Ciardi & Loeb 2000; Gou et al. 2004; Ioka & Mészáros 2005; Toma et al. 2010). As demonstrated in GRB 050904 by Subaru (Kawai et al. 2006; Totani et al. 2006), the GRBs can probe the interstellar neutral fraction with the Lyman  $\alpha$  red damp-

ing wing (Miralda-Escude 1998), the metal enrichment, and the star formation rate (Totani 1997; Kistler et al. 2009). In the future, we may also investigate the reionization history (Ioka 2003; Inoue 2004), the molecular history (Inoue et al. 2007), the equation of state of the Universe (Schaefer 2007; Yonetoku et al. 2004) and the extragalactic background light (Oh 2001; Inoue et al. 2010; Abdo et al. 2010).

The first stars are predicted to be predominantly very massive  $\gtrsim 100M_{\odot}$  (Abel et al. 2002; Bromm et al. 2002). The mass scale is roughly given by the Jeans mass (or Bonnor- Ebert mass) when the isothermality breaks (i.e., only through the cooling function) and hence seems robust (but see also Turk et al. 2009; Clark et al. 2010). The central part collapses first to a tiny ( $\sim 0.01M_{\odot}$ ) protostar, followed by the rapid accretion of the surrounding matter to form a massive first star (Omukai & Palla 2003; Yoshida et al. 2008). The stars with  $140\text{--}260M_{\odot}$  are expected to undergo the pair-instability supernovae without leaving any compact remnant behind, while those above  $\sim 260M_{\odot}$  would collapse to a massive ( $\sim 100M_{\odot}$ ) black hole with an accretion disk, potentially leading to scaled-up collapsar GRBs (Fryer et al. 2001; Heger et al. 2003; Suwa et al. 2007a,b, 2009; Komissarov & Barkov 2010; Mészáros & Rees 2010). The Pop III GRB rate would be rare  $\sim 0.1\text{--}10$  yr<sup>-1</sup> but within reach (e.g., Bromm & Loeb 2006; Naoz & Bromberg 2007). These GRBs also marks the formation of the first black holes, which may grow to the supermassive black holes (BHs) via merger or accretion (Madau & Rees 2001).

However, the zero-metal stars could have little mass loss by the line driven wind (Kudritzki 2002), and thereby have a large ( $R_* \sim 10^{13}$  cm) hydrogen envelope at the end of life (red supergiant (RSG) phase). Especially for Pop III stars, the mass accretion continues during the main sequence phase, so that the chemically homogeneous evolution induced by rapid rotation (e.g., Yoon & Langer 2005) might not work (Ohkubo et al.

<sup>1</sup> Department of Physics, School of Science, the University of Tokyo, 7-3-1 Hongo, Bunkyo-ku, Tokyo 113-0033, Japan

<sup>2</sup> Yukawa Institute for Theoretical Physics, Kyoto University, Oiwake-cho, Kitashirakawa, Sakyo-ku, Kyoto, 606-8502, Japan

<sup>3</sup> KEK Theory Center and the Graduate University for Advanced Studies (Sokendai), 1-1 Oho, Tsukuba 305-0801, Japan  
Electronic address: suwa@yukawa.kyoto-u.ac.jp

2009). Their extended envelopes may suppress the emergence of relativistic jets out of their surface even if such jets were produced (Matzner 2003). The observed burst duration  $T \sim 100$  s, providing an estimate for the lifetime of the central engine, suggests that the jet can only travel a distance of  $\sim cT \sim 10^{12}$  cm before being slowed down to a nonrelativistic speed. This picture is also supported by the nondetections of GRBs associated with type II supernovae. Nevertheless, this may not apply to the Pop III GRBs because the massive stellar accretion could enhance the jet luminosity and duration and therefore enable the jet to break out the first stars.

In this paper, we discuss the jet propagation in the first stars using the state-of-the-art Pop III stellar structure calculated by Ohkubo et al. (2009) (§ 2) to estimate the jet luminosity via accretion (§ 2,3) and to predict the observational main characters of the Pop III GRBs, such as energy and duration. We adopt the analytical approach that reproduces the previous numerical simulations to see the dependences on the yet uncertain stellar structure (§ 6 for analytical estimates) and to avoid simulations over many digits. We determine the jet head speed that is decelerated by the shock with the stellar matter (§ 4). The shocked matter is wasted as a cocoon surrounding the jet before the jet breakout (§ 5), like in the context of active galactic nuclei (Begelman & Cioffi 1989). We treat both the jet luminosity and its penetrability with the same stellar structure consistently for the first time.

## 2. PROGENITOR STRUCTURE

In this paper we employ three representative progenitors; Pop III star, Wolf-Rayet (WR) star, and RSG. These stars correspond to progenitors of Pop III GRBs, ordinary GRBs, and core-collapse supernovae without GRBs, respectively. The WR stars have no hydrogen envelope, which is a preferred condition for a successful jet break (Matzner 2003) and consistent with the observational evidence of GRB-SN Ibc association (Woosley & Bloom 2006).

The density profiles of investigated models are shown in Fig. 1. Red line shows the density profile of Pop III star with  $915 M_{\odot}$ , model Y-1 of Ohkubo et al. (2009). Blue indicates the GRB progenitor with  $16 M_{\odot}$ , model 16TI of Woosley & Heger (2006). Green line represents the progenitor of ordinary core-collapse supernovae with  $15 M_{\odot}$ , s15.0 of Woosley et al. (2002). The density profiles are roughly divided into two parts: core and envelope. The GRB progenitor (WR star) does not have hydrogen envelope, while Pop III and RSG keep their envelope so that these stars experience the envelope expansion triggered by core shrinkage after the main sequence.

Because the exact stellar surface is difficult to calculate for the simulation of stellar evolution (K. Nomoto, private communication), we numerically solve the equation of hydrostatic equilibrium,

$$\frac{\partial P}{\partial r} = -\frac{GM_r}{r^2}\rho, \quad (1)$$

for the outermost layer of stars, where  $P$  is the pressure,  $r$  is the radius from the center of the star,  $G$  is the gravitational constant,  $M_r$  is the mass inside  $r$ , and  $\rho$  is the density, respectively. We employ the polytropic equation of state,  $P = K\rho^\gamma$ , where  $K$  is the coefficient depending on the microphysics and  $\gamma$  is the adiabatic index. Here,

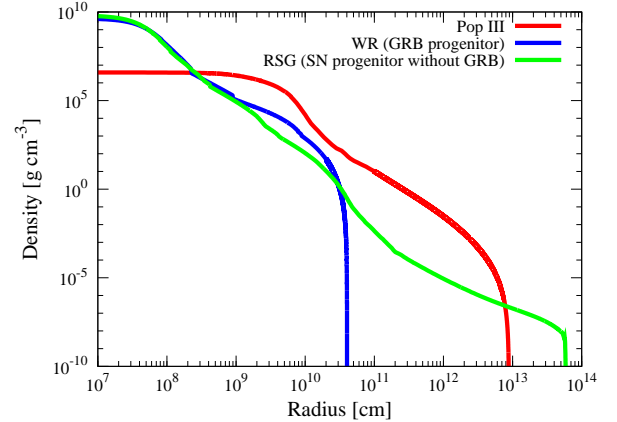


FIG. 1.— Density profiles of investigated models. Red, blue, and green lines correspond to Pop III star ( $M = 915M_{\odot}$ ), Wolf-Rayet star (WR; GRB progenitor,  $M = 16M_{\odot}$ ), and red supergiant (RSG; SN progenitor without GRB,  $M = 15M_{\odot}$ ), respectively. Pop III and RSG have a hydrogen envelope, which expands to a large radius, while WR has only a core.

we use the constant value of  $K$ , fitting just outside the core. The surfaces of stars are determined by the point with  $P = 0$ .

We can calculate the accretion rate,  $\dot{M}$ , using these density profiles. The accretion timescale of matter at a radius  $r$  to fall to the center of the star is roughly equal to the free-fall timescale,

$$t_{\text{ff}} \approx \sqrt{\frac{r^3}{GM_r}}. \quad (2)$$

Then we can evaluate the accretion rate at the center as  $\dot{M} = dM_r/dt_{\text{ff}}$ . Note that our estimation neglects the effect of rotation (e.g., Kumar et al. 2008; Perna & MacFadyen 2010). However the rotation law inside the star is very uncertain. Even though a rotationally supported disk is formed, the accretion time is roughly  $\sim \alpha^{-1} = 10(\alpha/0.1)^{-1}$  times  $t_{\text{ff}}$ , where  $\alpha$  is the standard dimensionless viscosity parameter (Kumar et al. 2008). In addition, the jet production mechanism is also unknown so that we introduce an efficiency parameter to connect the (free-fall) mass accretion rate and jet luminosity, which will be normalized by the observed GRBs in the next section. This parameter would contain the information of both the rotation rate and the jet production efficiency.

In Fig. 2, the mass accretion rates of investigated models are shown. The origin of time in this figure is set at the time of BH mass (central mass) being  $3M_{\odot}$  (3.4 sec after the onset of collapse for WR, for instance). The accretion rate should be related to the activity of the central engine, and that of Pop III stars is much larger than the other progenitors. Therefore, the GRBs of Pop III stars are expected to be more energetic than ordinary GRBs if Pop III stars could produce GRBs. However, it is nontrivial that the GRB jets can breakout the Pop III stars. In §4, we discuss the jet propagation and capability of successful jet break. The colored regions in this figure show the hidden regions by the stellar interior where the jet propagates inside the star so that the high energy photons can not be observed.

## 3. JET MODELS

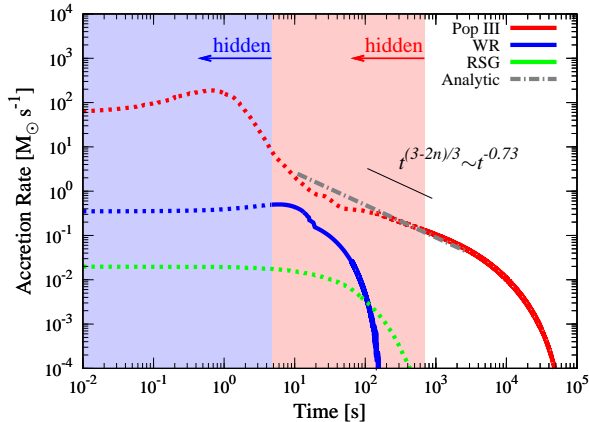


FIG. 2.— Accretion rates as a function of time. Red, blue, and green lines show Pop III, WR, and RSG, respectively. Dotted regions represent that the jet propagates inside the star, while the solid regions correspond to the time after the jet breakout for the magnetic jet model. Solid lines give information of observables (e.g., duration and energetics of GRB). On the other hand, dotted regions show the hidden energy inside the star that goes into the nonrelativistic cocoon component. The gray dot-dashed line represents the analytic model in Eq. (13). The black line shows  $t^{(3-2n)/3} \sim t^{-0.73}$  as a reference, where  $n \sim 2.6$  is a parameter for the density profile (an effective polytropic index of the envelope; see §6).

In this study we employ the *collapsar* model, which is a widely accepted scenario for the central engine of long GRBs. In this scenario a black hole accompanied by the stellar collapse produces a relativistic jet, which is strongly suggested by observations. The greatest uncertainty in this scenario is the mechanism for converting the accretion energy or BH rotation energy into the directed relativistic outflows. There are mainly two candidates of the jet production in the vicinity of the central engine: neutrino annihilation and magnetohydrodynamical (MHD) mechanisms including Blandford-Znajek process (Blandford & Znajek 1977), which converts the BH rotation energy into the Poynting flux jet via magnetic fields. Although there are plentiful studies about these mechanisms (e.g., Popham et al. 1999; Di Matteo et al. 2002; Proga et al. 2003; McKinney 2006), we have no concrete consensus for the available energy injection rate from the central engine into the jet. Therefore, we employ two simple models for jet producing mechanisms. We assume that the jet injection luminosity can be written with functions of the accretion rate,  $\dot{M}$ . The models used in this study is basically written in  $\dot{M}$  or  $\dot{M}^2$ . The accretion-to-jet efficiency are given by the GRB observables with the WR model in §5. More detailed expressions are following:

(A)  $L \sim \dot{M}$  model (MHD mechanism): A jet is driven by magnetic fields that are generated by accreting matter<sup>4</sup>. In this case the jet injection luminosity is given by  $L_j = \eta \dot{M} c^2$ , where  $\eta$  is the efficiency parameter. In Komissarov & Barkov (2010),  $\eta = 0.05/\alpha\beta$ , where  $\beta$  is the so-called plasma beta ( $\beta = 8\pi P/B^2$  with  $B$  being magnetic field), and we do not know the reliable values for both  $\alpha$  and  $\beta$  in the collapsar scenario. Therefore we

<sup>4</sup> Although the existence of strong magnetic field in the Pop III stars is unclear, there are several studies on the magnetic field amplification (e.g., Sur et al. 2010). Here we assume that the strong magnetic field can be generated at the vicinity of the BH.

parameterize these parameters with  $\eta$  simultaneously.

(B)  $L \sim \dot{M}^2$  model (neutrino-annihilation mechanism): A jet is driven by annihilation of neutrinos ( $\nu\bar{\nu} \rightarrow e^-e^+$ ), which are copiously radiated by “hyperaccretion flow” (MacFadyen & Woosley 1999). As for neutrino-annihilation process, the jet injection luminosity is written as  $L_j = \zeta \dot{M}^{9/4} M_{\text{BH}}^{-3/2}$  (Zalamea & Beloborodov 2010), where  $\zeta$  is the efficiency parameter including the information of accretion disk, e.g., the spectrum of emitted neutrinos and geometry of disk.

#### 4. PENETRATION OF STELLAR ENVELOPE

In this section, we consider the propagation of the jet head in the progenitor star. If a relativistic jet ( $\Gamma_j \gg 1$ ) strikes the stellar matter, two shocks are formed: a forward shock (FS) that accelerates the external material to a Lorentz factor  $\Gamma_h$ , and a reverse shock (RS) that decelerates the head of the jet to  $\Gamma_h$ . Balancing the energy density behind the FS ( $P_f$ ) with that above the RS ( $P_r$ ), one can obtain the Lorentz factor of the jet head. As for the ultra-relativistic case ( $\Gamma_h \gg 1$ ),  $P_f = \frac{4}{3}\Gamma_h^2 \rho c^2$  and  $P_r = \frac{4}{3}(\frac{\Gamma_j}{2\Gamma_h})^2 n_j m_p c^2$ , where  $n_j = L_{\text{iso}}/4\pi r^2 \Gamma_j^2 c$  is the jet proper proton density with  $L_{\text{iso}}$  being the isotropic luminosity of a jet and  $m_p$  is the proton mass, while for nonrelativistic case ( $\Gamma_h \approx 1$ ),  $P_f = \frac{\gamma+1}{2}\rho\beta_h^2 c^2$  and  $P_r = \frac{4}{3}\Gamma_j^2 n_j m_p c^2$ , where  $\beta_h$  is the velocity of FS in unit of the speed of light,  $c$ . These equations leads following relations: ultra-relativistic one,  $\Gamma_h \sim L_{\text{iso}}^{1/4} r^{-1/2} \rho^{-1/4}$  (Mészáros & Waxman 2001), and nonrelativistic one,  $\beta_h \sim L_{\text{iso}}^{1/2} r^{-1} \rho^{-1/2}$  (Waxman & Mészáros 2003). Here we combine these equations empirically as follows:

$$\beta_h \Gamma_h^2 \approx 18 \left( \frac{L_{\text{iso}}}{10^{52} \text{erg s}^{-1}} \right)^{1/2} \left( \frac{r}{10^{12} \text{cm}} \right)^{-1} \times \left( \frac{\rho}{10^{-7} \text{g cm}^{-3}} \right)^{-1/2}. \quad (3)$$

This approximation leads the same relation with Waxman & Mészáros (2003) for the nonrelativistic case ( $\Gamma_h \approx 1$ ) and agree with Mészáros & Waxman (2001) to within 40% for the ultra-relativistic case ( $\beta_h \approx 1$ ). The crossing time of the FS is also given by

$$t_h \approx \frac{r}{\Gamma_h^2 \beta_h c}. \quad (4)$$

As for the relativistic FS, the crossing time is much shorter than the light crossing time due to its large Lorentz factor (see Mészáros & Rees 2001).

Combining Eqs. (3) and (4), we obtain the necessary isotropic jet luminosity for the FS to reach the radius  $r$  as

$$L_{\text{iso}} \approx 3 \times 10^{52} \left( \frac{r}{10^{12} \text{cm}} \right)^4 \left( \frac{\rho}{10^{-7} \text{g cm}^{-3}} \right) \times \left( \frac{t}{1 \text{s}} \right)^{-2} \text{erg s}^{-1}. \quad (5)$$

If the jet luminosity decreases slower than  $t^{-2}$ , the jet luminosity can achieve this value at the late phase. We can follow the evolution of the FS by equating  $L_j$  and Eq. (5) including the correction of the jet opening angle,  $\theta_j$  (i.e.,  $L_j = L_{\text{iso}} \theta_j^2/2$ ).



We note that the accreting gas from the surrounding to the progenitor star is negligible for the jet breakout since the density of the accreting gas is low,  $\rho = \dot{M}/4\pi r^2 v \sim 5 \times 10^{-12} \text{ g cm}^{-3} (\dot{M}/10^{-2} M_\odot \text{ yr}^{-1}) (r/10^{13} \text{ cm})^{-2} (v/10^8 \text{ cm s}^{-1})^{-1}$ .

## 5. GRB AND COCOON

In this section, we divide the energetics of the jet into two components: GRB emitter (relativistic component) and cocoon (nonrelativistic component). When the Lorentz factor of the FS,  $\Gamma_h$ , is smaller than  $\theta_j^{-1}$ , the shocked material may escape sideways and form the cocoon (Matzner 2003), which avoids the baryon loading problem. With this scenario, the injected energy before the shock breakout goes to the energy of cocoon and that after breakout goes to the GRB emitter. Therefore, we can calculate the energy budget of the GRB emitter and cocoon after the determination of the jet breakout time,  $t_b$ . We define  $t_b$  as the maximum time obtained by Eq. (5).

First of all, we determine the accretion-to-jet conversion efficiency (depending on the mechanism) using the ordinary GRB progenitor (WR) to make the total energy of GRB emitter  $E_{\text{tot}} = 10^{52} \text{ erg}^5$ . In this estimation we assume that the half opening angle of the jet  $\theta_j = 5^\circ$ . A successful GRB requires following two conditions; i) The jet head reaches the stellar surface. ii) The velocity of the jet head,  $\beta_h$ , should be larger than that of the cocoon,  $\beta_c$  (Matzner 2003; Toma et al. 2007).

As for  $L \sim \dot{M}$  model, the results of the WR case are  $L_j = 1.1 \times 10^{51} (\dot{M}/M_\odot \text{ s}^{-1}) \text{ erg s}^{-1}$ , i.e.,

$$\eta = \frac{L_j}{\dot{M}c^2} \approx 6.2 \times 10^{-4}, \quad (6)$$

and  $t_b = 4.7 \text{ s}$ . For  $L \sim \dot{M}^2$  model,  $L_j = 76 \times 10^{51} (\dot{M}/M_\odot \text{ s}^{-1})^{9/4} (M_{\text{BH}}/M_\odot)^{-3/2} \text{ erg s}^{-1}$  and  $t_b = 2.8 \text{ s}^6$ . We estimate the expected duration of the burst with the period during which 90 percent of the burst's energy is emitted,  $T_{90}$ . Both models reproduce the typical duration of burst of  $\sim 10 \text{ s}$  (see Table 1). The energy of cocoon (injected energy before the shock breakout) is smaller than that of the GRB emitter. The isotropic kinetic energy of the GRB emitter is  $\sim 10^{54} \text{ erg}$ .

Next, we apply the above scheme and jet luminosity (e.g., the same  $\eta$  and  $\zeta$ ) to the RSG (progenitor of supernovae without GRBs) and find that RSG can not produce GRB. This is because the jet head is slower than the cocoon. As for WR with  $L \sim \dot{M}$  model,  $\beta_h \sim R_*/(ct_b) \sim 0.3$  and  $\beta_c \sim \sqrt{E_c/(Mc^2)} \sim 0.01$ , where  $E_c \sim 2 \times 10^{51} \text{ erg}$  is the energy of the cocoon (see Table 1) and  $M \sim 10M_\odot$  is the stellar mass, hence  $\beta_h > \beta_c$ . On the other hand,  $\beta_h \sim 0.007$  and  $\beta_c \sim 0.01$ , i.e.  $\beta_h \lesssim \beta_c$ , for the RSG. Thus the morphology of the shock wave is almost spherical and the jet cannot break

<sup>5</sup> Note that  $E_{\text{tot}}$  is not the total energy of gamma rays because there must be a conversion from the jet kinetic energy to gamma rays. Though the efficiency of conversion is unclear, it is typically the order of 0.1. Therefore, we employ  $E_{\text{tot}} = 10^{52} \text{ erg}$  that could lead the true gamma-ray energy of GRB  $\sim 10^{51} \text{ erg}$ .

<sup>6</sup> This luminosity shows a similar value with Eq. (22) of Zalamea & Beloborodov (2010) because if  $M_{\text{BH}} = 3M_\odot$ ,  $L_j \approx 16 \times 10^{51} \text{ erg s}^{-1}$ .

out the stellar surface with a small opening angle. In addition, the FS cannot reach the stellar surface with  $L \sim \dot{M}^2$  model for the RSG. Therefore our scheme is consistent with observations of GRB-SN Ibc connection.

Finally, we calculate the evolution of the jet head for the case of Pop III star (see Table 1). We find that the  $L \sim \dot{M}^2$  model does *not* produce GRB because the FS stalls inside the envelope due to rapidly decreasing jet luminosity (so-called ‘‘failed GRB’’). On the other hand, the  $L \sim \dot{M}$  model can supply enough energy for a jet to penetrate the envelope and produce a GRB. Since  $\beta_h \sim 0.4$  and  $\beta_c \sim 0.08$  in this model, the relativistic jet can penetrate the stellar envelope with a small opening angle and produce a successful GRB. The total energy of the GRB jet (injected energy after breakout) is  $\sim 45$  times larger than the ordinary GRB and the duration is much longer ( $T_{90} \sim 1000 \text{ s}$ ). In addition, we estimate the minimum  $\eta$  for the successful breakout, which is  $\eta \approx 3.4 \times 10^{-5}$ . This is 20 times smaller than that of the normal GRB. In this case  $\beta_h \sim 0.03$  and  $\beta_c \sim 0.008$ . Below this value, the jet head cannot reach the stellar surface.

The accretion of the envelope (not core) is very important for the Pop III GRB. Although the envelope is mildly bounded by the gravitational potential (because  $\gamma \approx 1.38 \sim 4/3$ ) and easily escapes when it is heated by the shock, the timescale of cocoon passing in the envelope ( $\sim R_*/(c\beta_c) \sim 3000 \text{ s}$ ) is longer than  $t_b$ . Therefore, the envelope accretion can last till the jet breakout and our conclusion about the penetrability of the relativistic jet is not changed.

It should be noted that the opening angle of the jet could not be constant during the propagation phase. Due to the additional collimation by the gas pressure,  $\theta_j$  becomes smaller as the jet propagates (e.g., Zhang et al. 2003; Mizuta et al. 2006, 2010). The smaller  $\theta_j$  leads the larger  $L_{\text{iso}} (= 2L_j/\theta_j^2)$  so that our constant  $\theta_j$  is a conservative assumption for the jet breakout.

## 6. ANALYTICAL DEPENDENCES ON PARAMETERS

The hydrogen envelope could be reduced by the mass loss, which is one of the most uncertain processes in the stellar evolution. Even in the zero-metal stars, the synthesized heavy element could be dredged up to the surface, and might induce the line driven wind. The stellar luminosity could also exceed the Eddington luminosity of the envelope. The stellar pulsation might also blow away the envelope dynamically. So we analytically estimate the dependence on the envelope mass in the following.

The density profile of the envelope can be written as

$$\rho(r) \approx \rho_1 \left( \frac{R_*}{r} - 1 \right)^n, \quad (7)$$

where  $n$  is a constant (Matzner & McKee 1999). This profile is exact if the enclosed mass is constant (i.e., the envelope mass is negligible compared with the core mass) and the equation of state is polytropic, in which case  $n = (\gamma - 1)^{-1}$  is a polytropic index. We have  $n = 3/2$  for efficiently convective envelopes since the adiabatic index is  $\gamma = 5/3$  for the ideal monoatomic gas, and  $n = 3$  for radiative envelopes of constant opacity  $\kappa$  since  $P \propto \rho^{4/3}$  is derived from the relations,  $P_\gamma = (L/L_{\text{Edd}})P$ ,  $P \propto \rho T$ ,  $P_\gamma \propto T^4$ , with a constant luminosity-mass ratio  $L/M$

where  $L_{\text{Edd}} = 4\pi GMc/\kappa > L$  is the Eddington luminosity. We can fit well the Pop III envelope in Fig. 1 with  $n \approx 2.6$ .

Using the profile in equation (7), we can estimate the envelope mass as

$$M_{\text{env}} = \int_{R_c}^{R_*} \rho(r) 4\pi r^2 dr \propto \frac{\rho_1 R_*^3}{3-n} \sim \frac{\rho_c R_c^n R_*^{3-n}}{3-n}, \quad (8)$$

where  $\rho_c \equiv \rho(R_c) \approx \rho_1 (R_*/R_c)^n$  is the envelope density just above the core and  $R_c$  is the core radius. The core density is higher than  $\rho_c$  to proceed with the nuclear burning. Since the density enhancement is determined by the difference of the ignition temperature, which is not sensitive to other parameters, we assume that the core mass is given by  $M_c \propto \rho_c R_c^3$ , so that

$$M_{\text{env}} \propto \frac{M_c R_c^{n-3} R_*^{3-n}}{3-n}. \quad (9)$$

Then the stellar radius can be written as a function of the core radius, the core mass, and the envelope mass as follows:

$$R_* \sim 10^{13} \text{ cm} \left( \frac{R_c}{10^{10} \text{ cm}} \right) \left( \frac{M_c}{400 M_\odot} \right)^{-2.5} \times \left( \frac{M_{\text{env}}}{500 M_\odot} \right)^{2.5}, \quad (10)$$

where we use  $n = 2.6$  (see Appendix for  $n$  dependences). Therefore, the stellar radius has a strong dependence on the envelope mass. If the envelope mass is smaller than  $\sim 50 M_\odot$ , the stellar radius is almost the core radius,  $R_c \sim 10^{10}$  cm.

Next, we consider the jet breakout time. Since the accretion time of the core ( $r \lesssim 10^{10}$  cm) is  $\sim 4$  s, the envelope accretion is important for the successful breakout if  $t_b$  is longer than this timescale. Using  $t_{\text{ff}} \sim \sqrt{r^3/GM_r}$ , we can evaluate the envelope accretion rate as

$$\dot{M} = \frac{dM_r/dr}{dt_{\text{ff}}/dr} \propto \rho_1 M_c^{(3-n)/3} R_*^n t^{(3-2n)/3} \quad (11)$$

with the approximation of  $M_r - M_c = \int_{R_c}^r \rho(r') 4\pi r'^2 dr' \ll M_c \approx 400 M_\odot$ , which is valid for  $r \lesssim 10^{12}$  cm (corresponding to  $t_{\text{ff}} \lesssim 3000$  s). Combining with Eqs. (5), (10), (11) and  $L_j = \eta \dot{M} c^2 = L_{\text{iso}} \theta_j^2/2$ , the breakout time is given by

$$t_b \sim 700 \text{ s} \left( \frac{\eta}{10^{-3}} \right)^{-0.79} \left( \frac{\theta_j}{5^\circ} \right)^{1.6} \left( \frac{R_c}{10^{10} \text{ cm}} \right)^{1.1} \times \left( \frac{M_c}{400 M_\odot} \right)^{-2.9} \left( \frac{M_{\text{env}}}{500 M_\odot} \right)^{2.8}, \quad (12)$$

where we use  $n = 2.6$  (see Appendix for  $n$  dependences) and put  $\rho = \rho_1$  and  $r = R_*$  in Eq. (5). If  $\eta$  is very small ( $\lesssim 10^{-5}$ ) and  $t_b$  is longer than the free-fall timescale of the outermost part of star ( $\sim 10^5$  s), the jet cannot penetrate the star. When  $\eta \approx 10^{-5}$ ,  $\beta_h \sim R_*/t_b \sim 0.003$  and  $\beta_c \sim \sqrt{\eta} \sim 0.003$  so that the shock wave also propagates almost spherically. Similarly, the RSG case in Fig. 2 also has too long breakout time since  $M_c \sim 4 M_\odot$  and  $M_{\text{env}} \sim 11 M_\odot$ .

The jet luminosity after the breakout ( $t > t_b$ ) is given by

$$L_{\text{iso}}(t) \sim 5 \times 10^{52} \left( \frac{\eta}{10^{-3}} \right) \left( \frac{\theta_j}{5^\circ} \right)^{-2} \left( \frac{R_c}{10^{10} \text{ cm}} \right)^{-0.4} \times \left( \frac{M_c}{400 M_\odot} \right)^{1.1} \left( \frac{t}{700 \text{ s}} \right)^{-0.73} \text{ erg s}^{-1}, \quad (13)$$

where we use  $n = 2.6$  (see Appendix for  $n$  dependences) and  $M_c \propto \rho_c R_c^3 \sim \rho_1 (R_*/R_c)^n R_c^3$ . Interestingly the dependence of  $L_{\text{iso}}(t)$  on the envelope mass is only through the time,  $t$ . The relativistic jet emitted after the breakout will produce GRB prompt emission and the jet luminosity decreases with time as  $t^{-(2n-3)/3} \sim t^{-0.73}$  in this case. Fig. 2 shows this dependence with the gray dot-dashed line, which well reproduces the numerical result (red line) for  $10 \text{ s} \lesssim t \lesssim 3000 \text{ s}$ . The parameter dependences just after the breakout (most luminous time;  $t = t_b$ ) are given by Eqs. (12) and (13) as

$$L_{\text{iso}}(t = t_b) \sim 5 \times 10^{52} \left( \frac{\eta}{10^{-3}} \right)^{1.6} \left( \frac{\theta_j}{5^\circ} \right)^{-3.2} \left( \frac{R_c}{10^{10} \text{ cm}} \right)^{-1.2} \times \left( \frac{M_c}{400 M_\odot} \right)^{3.2} \left( \frac{M_{\text{env}}}{500 M_\odot} \right)^{-2.0} \text{ erg s}^{-1}, \quad (14)$$

where we use  $n = 2.6$  (see also Appendix).

The active duration of the central engine ( $\approx t_b + T_{90}$ ) is determined by the accretion timescale at  $r \sim 10^{12}$  cm, where the density gradient gets larger because  $\rho(r) \propto (R_*/r - 1)^n$ . The region of  $r \lesssim 10^{12}$  cm has  $\rho(r) \propto (R_*/r)^n$  so that Eqs. (12) and (13) are valid, while they are not appropriate for  $r \gtrsim 10^{12}$  cm ( $M_r \gtrsim M_c + 0.4 M_{\text{env}}$ ) due to the existence of the stellar surface, which leads the fast decrease of the accretion rate (compare the red and gray lines in Fig. 2). So, the duration can be calculated by  $t_{\text{ff}}$  at  $r \sim 0.1 R_*$  with Eq. (10) as

$$t_{\text{ff}}(r = 0.1 R_*) \sim 3000 \left( \frac{R_c}{10^{10} \text{ cm}} \right)^{1.5} \left( \frac{M_c}{400 M_\odot} \right)^{-3.8} \times \left( \frac{M_{\text{env}}}{500 M_\odot} \right)^{3.8} \left( \frac{M_c + 0.4 M_{\text{env}}}{600 M_\odot} \right)^{-0.5} \text{ s}, \quad (15)$$

where we use  $n = 2.6$  (see also Appendix). This is consistent with the result  $t_b + T_{90} \sim 2200$  s in the previous section. At this time, the isotropic luminosity in Eq. (13) is given by

$$L_{\text{iso}}[t = t_{\text{ff}}(r = 0.1 R_*)] \sim 2 \times 10^{52} \left( \frac{\eta}{10^{-3}} \right) \left( \frac{\theta_j}{5^\circ} \right)^{-2} \times \left( \frac{R_c}{10^{10} \text{ cm}} \right)^{-1.5} \left( \frac{M_c}{400 M_\odot} \right)^{3.9} \left( \frac{M_{\text{env}}}{500 M_\odot} \right)^{-2.8} \times \left( \frac{M_c + 0.4 M_{\text{env}}}{600 M_\odot} \right)^{0.37} \text{ erg s}^{-1}, \quad (16)$$

where we use  $n = 2.6$  (see also Appendix). We note that the observables in Eqs. (14), (15) and (16) carry information of the stellar structure.

## 7. SUMMARY AND DISCUSSION

We have investigated the jet propagation in the very massive Population III stars assuming the accretion-to-jet conversion efficiency of the observed normal GRBs.

We find that the jet can potentially break out the stellar surface even if the Pop III star has a massive hydrogen envelope thanks to the long-lasting accretion of the envelope itself. Even if the accretion-to-jet conversion is less efficient than the ordinary GRBs by a factor of  $\sim 20$ , the jet head can penetrate the stellar envelope and produce GRBs. Although the total energy injected by the jet is as large as  $\sim 10^{54}$  erg, more than half is hidden in the stellar interior and the energy injected before the breakout goes into the cocoon component. The large envelope accretion can activate the central engine so that the duration of Pop III GRB is very long if the hydrogen envelope exists. As a result, the luminosity of Pop III GRB is modest, being comparable to that of ordinary GRBs.

Considering the Pop III GRB at redshift  $z$ , the duration in Eq. (15) is

$$T_{\text{GRB}} = T_{90}(1+z) \approx 30000 \text{ s} \left( \frac{1+z}{20} \right), \quad (17)$$

which is much longer than the canonical duration of GRBs,  $\sim 20$  s. The total isotropic-equivalent energy of Pop III GRB is

$$E_{\gamma, \text{iso}} = \varepsilon_{\gamma} E_{\text{iso}} \approx 1.2 \times 10^{55} \left( \frac{\varepsilon_{\gamma}}{0.1} \right) \text{ erg}, \quad (18)$$

where  $\varepsilon_{\gamma}$  is the conversion efficiency from the jet kinetic energy to gamma rays (see Table 1). It should be noted that this value is comparable to the largest  $E_{\gamma, \text{iso}}$  ever observed,  $\approx 9 \times 10^{54}$  erg for GRB 080916C (Abdo et al. 2009). This value is smaller than the estimation of Komissarov & Barkov (2010); Mészáros & Rees (2010) because we consider the hidden (cocoon) component. Since the large isotropic energy is stretched over the long duration, the expected flux just after the breakout is not so bright,

$$F = \frac{\varepsilon_{\gamma} L_{\text{iso}}}{4\pi r_L^2} \sim 10^{-9} \text{ erg cm}^{-2} \text{ s}^{-1}, \quad (19)$$

where  $r_L$  is the luminosity distance, which is smaller than the *Swift* Burst Array Telescope (BAT) sensitivity,  $\sim 10^{-8}$  erg cm $^{-2}$  s $^{-1}$ . However, there must be a large variety of the luminosity as ordinary GRBs so that more luminous but rare events might be observable by BAT. Although the cocoon component has a large energy, the velocity is so low that it is also difficult to observe. If the cocoon component interacts with the dense wind or

ambient medium, it might be observable. This is an interesting future work.

The above discussions strongly depend on the envelope mass because the stellar radius is highly sensitive to the envelope mass. We derive analytical dependences on the model parameters in § 6, which are applicable to a wide variety of progenitor models. According to the analytical estimates, the smaller envelope leads to the shorter duration and the larger observable luminosity. If  $M_{\text{env}} \lesssim 50M_{\odot}$ ,  $R_* \sim R_c \sim 10^{10}$  cm (see Eq.(10)),  $t_b \sim 2$  s (obtained using numerical model as in §5), and  $T_{90} \sim t_{\text{ff}} \sim 4(M/400M_{\odot})^{-1/2}(R_c/10^{10}\text{cm})^{3/2}$  s; Both  $t_b$  and  $T_{90}$  might be extended by a factor of  $\alpha^{-1}$  due to the rotation. This is much shorter than the GRBs from Pop III stars with massive envelopes. The mass accreting after the breakout is  $\sim 200M_{\odot}$  so that  $E_{\gamma, \text{iso}} \sim 3 \times 10^{54}(\varepsilon_{\gamma}/0.1)$  erg can be emitted by gamma rays after breakout. The luminosity just after the breakout is  $L_{\text{iso}} \sim 10^{54}$  erg s $^{-1}$ , i.e.,  $F \sim 10^{-7}$  erg cm $^{-2}$  s $^{-1}$ , which is much brighter than the case with the massive envelope and observable with the *Swift* BAT, while the duration is very short ( $\sim 2$  s at the source frame).

The matter entrainment from the envelope is also crucial for the fireball dynamics and the GRB spectra (e.g., Ioka 2010). Since the envelope of the PopIII star is different from that of present-day stars, the GRB appearance is also likely distinct from the observed ones. This is also an interesting future work.

Since we do not have any conclusive central engine scenario, we employ two popular mechanisms in this paper, that is, the magnetic model ( $L \sim \dot{M}$ ) and neutrino-annihilation model ( $L \sim \dot{M}^2$ ). The difference between these models is the dependence of the mass accretion rate. We find that the neutrino-annihilation model cannot penetrate the Pop III stellar envelope, so that no GRB occurs, which is consistent with Fryer et al. (2001); Komissarov & Barkov (2010); Mészáros & Rees (2010).

We would like to thank A. Heger and T. Ohkubo for providing the progenitor models and P. Mészáros and K. Omukai for valuable discussions. This study was supported in part by the Japan Society for Promotion of Science (JSPS) Research Fellowships (YS) and by the Grant-in-Aid from the Ministry of Education, Culture, Sports, Science and Technology (MEXT) of Japan (No.19047004, 21684014, 22244019).

## APPENDIX

### DEPENDENCE ON THE DENSITY INDEX $n$

Here we explicitly show the dependences on  $n$  in Eqs. (10), (12), (13), (14), (15) and (16) as follows,

$$R_* \propto R_c M_c^{-\frac{1}{3-n}} [(3-n)M_{\text{env}}]^{\frac{1}{3-n}}, \quad (A1)$$

$$t_b \propto \eta^{-\frac{3}{9-2n}} \theta_j^{\frac{6}{9-2n}} R_c^{\frac{3(4-n)}{9-2n}} M_c^{-\frac{n^2-9n+21}{(3-n)(9-2n)}} [(3-n)M_{\text{env}}]^{\frac{3(4-n)}{(3-n)(9-2n)}}, \quad (A2)$$

$$L_{\text{iso}}(t) \propto \eta \theta_j^{-2} R_c^{-(3-n)} M_c^{\frac{6-n}{3}} t^{-\frac{2n-3}{3}}, \quad (A3)$$

$$L_{\text{iso}}(t = t_b) \propto \eta^{\frac{6}{9-2n}} \theta_j^{-\frac{12}{9-2n}} R_c^{-\frac{15-4n}{9-2n}} M_c^{\frac{2n^2-16n+33}{(3-n)(9-2n)}} [(3-n)M_{\text{env}}]^{-\frac{(4-n)(2n-3)}{(3-n)(9-2n)}}, \quad (A4)$$

$$t_{\text{ff}}(r = 0.1R_*) \propto R_c^{\frac{3}{2}} M_c^{-\frac{3}{2(3-n)}} [(3-n)M_{\text{env}}]^{\frac{3}{2(3-n)}} (M_c + 0.4M_{\text{env}})^{-\frac{1}{2}}, \quad (A5)$$

$$L_{\text{iso}}[t = t_{\text{ff}}(r = 0.1R_*)] \propto \eta \theta_j^{-2} R_c^{-\frac{3}{2}} M_c^{\frac{2n^2-12n+27}{6(3-n)}} [(3-n)M_{\text{env}}]^{\frac{3-2n}{2(3-n)}} (M_c + 0.4M_{\text{env}})^{\frac{2n-3}{6}}. \quad (A6)$$

TABLE 1  
MODEL SUMMARY

Model (Reference)	Final Mass [ $M_{\odot}$ ]	Radius [ $10^{11}$ cm]	Mechanism	$t_b$ [s]	Energy of GRB emitter [ $10^{52}$ erg]	Energy of Cocoon [ $10^{52}$ erg]	$T_{90}$ [s]	$E_{\text{iso}}$ [ $10^{54}$ erg]
WR (Woosley & Heger 2006)	14	0.4	MHD Neutrino	4.7 2.8	1.0 1.0	0.23 0.42	49 10	2.6 2.6
Pop III (Ohkubo et al. 2009)	915	90	MHD Neutrino	690 —	45 —	57 —	1500 —	120 —
RSG (Woosley et al. 2002)	13	600	MHD Neutrino	$(5 \times 10^5)$ —	(0.88) —	(0.16) —	$(8.4 \times 10^6)$ —	— —

NOTE. — The final masses of WR and RSG are not the same mass as the initial mass of progenitors ( $15M_{\odot}$  and  $16M_{\odot}$ ) because of mass loss due to stellar wind, while Pop III stars do not have mass loss so that the final mass is  $915M_{\odot}$ .  $t_b$  is the time of shock breakout from our calculations (see § 5). The energy of GRB emitter is the *kinetic* energy of relativistic jet after the breakout. The energy of the cocoon is the injected energy before the breakout.  $E_{\text{iso}}$  is the isotropic energy of GRB emitter, corrected by the half opening angle of the jet,  $\theta_j = 5^\circ$ . The parenthetic values for RSG are just for references because the cocoon velocity is larger than GRB emitter so that the GRB is not generated.

We note that the total energy is proportional to

$$t_{\text{ff}}(r = 0.1R_*)L_{\text{iso}}[t = t_{\text{ff}}(r = 0.1R_*)] \propto \eta\theta_j^{-2}M_c^{\frac{3-n}{3}}[(3-n)M_{\text{env}}](M_c + 0.4M_{\text{env}})^{-\frac{3-n}{3}}. \quad (\text{A7})$$

if  $n < 3$  (i.e.,  $L_{\text{iso}}(t)$  is shallower than  $t^{-1}$ ).

#### REFERENCES

- Abdo, A. A., et al. 2009, *Science*, 323, 1688  
 Abdo, A. A., et al. 2010, arXiv:1005.0996  
 Abel, T., Bryan, G. L., & Norman, M. L. 2002, *Science*, 295, 93  
 Barkana, R., & Loeb, A. 2001, *Phys. Rep.*, 349, 125  
 Begelman, M. C., & Cioffi, D. F. 1989, *ApJ*, 345, L21  
 Blandford, R. D., & Znajek, R. L. 1977, *MNRAS*, 179, 433  
 Bromm, V., Coppi, P. S., & Larson, R. B. 2002, *ApJ*, 564, 23  
 Bromm, V., & Larson, R. B. 2004, *ARA&A*, 42, 79  
 Bromm, V., & Loeb, A. 2006, *ApJ*, 642, 382  
 Chandra, P., et al. 2010, *ApJ*, 712, L31  
 Ciardi, B., & Ferrara, A. 2005, *Space Science Reviews*, 116, 625  
 Ciardi, B., & Loeb, A. 2000, *ApJ*, 540, 687  
 Clark, P. C., Glover, S. C. O., Klessen, R. S., & Bromm, V. 2010, arXiv:1006.1508  
 Di Matteo, T., Perna, R., & Narayan, R. 2002, *ApJ*, 579, 706  
 Fryer, C. L., Woosley, S. E., & Heger, A. 2001, *ApJ*, 550, 372  
 Gou, L. J., Mészáros, P., Abel, T., & Zhang, B. 2004, *ApJ*, 604, 508  
 Greiner, J., et al. 2009, *ApJ*, 693, 1610  
 Heger, A., Fryer, C. L., Woosley, S. E., Langer, N., & Hartmann, D. H. 2003, *ApJ*, 591, 288  
 Inoue, S. 2004, *MNRAS*, 348, 999  
 Inoue, S., Omukai, K., & Ciardi, B. 2007, *MNRAS*, 380, 1715  
 Inoue, S., Salvaterra, R., Choudhury, T. R., Ferrara, A., Ciardi, B., & Schneider, R. 2010, *MNRAS*, 404, 1938  
 Ioka, K. 2003, *ApJ*, 598, L79  
 —. 2010, *Progress of Theoretical Physics*, 124, 667  
 Ioka, K., & Mészáros, P. 2005, *ApJ*, 619, 684  
 Kawai, N., et al. 2006, *Nature*, 440, 184  
 Kistler, M. D., Yüksel, H., Beacom, J. F., Hopkins, A. M., & Wyithe, J. S. B. 2009, *ApJ*, 705, L104  
 Komissarov, S. S., & Barkov, M. V. 2010, *MNRAS*, 402, L25  
 Kudritzki, R. P. 2002, *ApJ*, 577, 389  
 Kumar, P., Narayan, R., & Johnson, J. L. 2008, *Science*, 321, 376  
 Lamb, D. Q., & Reichart, D. E. 2000, *ApJ*, 536, 1  
 MacFadyen, A. I., & Woosley, S. E. 1999, *ApJ*, 524, 262  
 Madau, P., & Rees, M. J. 2001, *ApJ*, 551, L27  
 Matzner, C. D. 2003, *MNRAS*, 345, 575  
 Matzner, C. D., & McKee, C. F. 1999, *ApJ*, 510, 379  
 McKinney, J. C. 2006, *MNRAS*, 368, 1561  
 Mészáros, P., & Rees, M. J. 2001, *ApJ*, 556, L37  
 —. 2010, *ApJ*, 715, 967  
 Mészáros, P., & Waxman, E. 2001, *Physical Review Letters*, 87, 171102  
 Miralda-Escude, J. 1998, *ApJ*, 501, 15  
 Mizuta, A., Nagataki, S., & Aoi, J. 2010, arXiv:1006.2440  
 Mizuta, A., Yamasaki, T., Nagataki, S., & Mineshige, S. 2006, *ApJ*, 651, 960  
 Naoz, S., & Bromberg, O. 2007, *MNRAS*, 380, 757  
 Oh, S. P. 2001, *ApJ*, 553, 25  
 Ohkubo, T., Nomoto, K., Umeda, H., Yoshida, N., & Tsuruta, S. 2009, *ApJ*, 706, 1184  
 Omukai, K., & Palla, F. 2003, *ApJ*, 589, 677  
 Perna, R., & MacFadyen, A. 2010, *ApJ*, 710, L103  
 Popham, R., Woosley, S. E., & Fryer, C. 1999, *ApJ*, 518, 356  
 Proga, D., MacFadyen, A. I., Armitage, P. J., & Begelman, M. C. 2003, *ApJ*, 599, L5  
 Salvaterra, R., et al. 2009, *Nature*, 461, 1258  
 Schaefer, B. E. 2007, *ApJ*, 660, 16  
 Sur, S., Schleicher, D. R. G., Banerjee, R., Federrath, C., & Klessen, R. S. 2010, arXiv:1008.3481  
 Suwa, Y., Takiwaki, T., Kotake, K., & Sato, K. 2007a, *ApJ*, 665, L43  
 —. 2007b, *PASJ*, 59, 771  
 —. 2009, *ApJ*, 690, 913  
 Tanvir, N. R., et al. 2009, *Nature*, 461, 1254  
 Toma, K., Ioka, K., Sakamoto, T., & Nakamura, T. 2007, *ApJ*, 659, 1420  
 Toma, K., Sakamoto, T., & Meszaros, P. 2010, arXiv:1008.1269  
 Totani, T. 1997, *ApJ*, 486, L71  
 Totani, T., Kawai, N., Kosugi, G., Aoki, K., Yamada, T., Iye, M., Ohta, K., & Hattori, T. 2006, *PASJ*, 58, 485  
 Turk, M. J., Abel, T., & O’Shea, B. 2009, *Science*, 325, 601  
 Waxman, E., & Mészáros, P. 2003, *ApJ*, 584, 390  
 Woosley, S. E., & Bloom, J. S. 2006, *ARA&A*, 44, 507  
 Woosley, S. E., & Heger, A. 2006, *ApJ*, 637, 914  
 Woosley, S. E., Heger, A., & Weaver, T. A. 2002, *Reviews of Modern Physics*, 74, 1015  
 Yonetoku, D., Murakami, T., Nakamura, T., Yamazaki, R., Inoue, A. K., & Ioka, K. 2004, *ApJ*, 609, 935  
 Yoon, S.-C., & Langer, N. 2005, *Astronomy and Astrophysics*, 443, 643  
 Yoshida, N., Omukai, K., & Hernquist, L. 2008, *Science*, 321, 669  
 Zalamea, I., & Beloborodov, A. M. 2010, arXiv:1003.0710  
 Zhang, W., Woosley, S. E., & MacFadyen, A. I. 2003, *ApJ*, 586, 356